Performance of adaptive transmit diversity with orthogonal space-time block coding in microcell and macrocell channel environments

Mahmoud, Seedahmed; Lin, Kevin; Hussain, Zahir

Performance of Adaptive Transmit Diversity with Orthogonal Space-Time Block Coding in Microcell and Macrocell Channel Environments

Seedahmed S. Mahmoud, Kevin H. Lin, and Zahir M. Hussain
School of Electrical and Computer Engineering, RMIT University, Melbourne, Victoria 3000, Australia
Emails: mahmoud.seedahmed@rmit.edu.au; s9510490@student.rmit.edu.au; zmhussain@ieee.org

Abstract— **Recently an adaptive transmit eigenbeamforming with orthogonal space-time block coding (Eigen-OSTBC) has been proposed. This model was simulated over macrocell environment with a uniform linear array (ULA) at the base station (BS). In this paper we investigate the impact of various antenna geometries on the performance of this scheme as well as the performance over microcell and macrocell channel environments. The geometrical-based hyperbolically distributed scatterers (GB-HDS) channel models were simulated with angular spreads (AS) taken from experimental data. The ULA and the uniform circular array (UCA) are considered at the BS. In the simulation conducted, results have shown that the Eigen-OSTBC system has a higher performance gain than OSTBC systems in macrocell than microcell environment (where the AS gets larger). It is also observed that BS antenna array with different separation distances also affects the performance of both Eigen-OSTBC and OSTBC systems. However, the error-rate performance curves of ULA and UCA configurations are very similar.**

I. INTRODUCTION

As communication systems have progressively increased in complexity, many new transmit diversity schemes have been devised and investigated to improve the error-rate performance and increase the capacity. In fact a number of researches have been conducted around the world to find a new wireless transmission techniques that can enhance both error performance and spectral efficiency. Amount these research efforts, spatial diversity transmission scheme (that takes an advantage of additional propagation paths in a multi-input multi-output (MIMO) system) has emerged as one of the promising techniques [1] - [3]. However, their performance improvement are based on the assumption that the arriving multipath signals are sufficiently uncorrelated. In cellular communications, due to close spacing between antenna elements at the base station (BS), signal paths are often correlated to some degree. As a consequence, coherent deep fade between propagation signal paths is unavoidable and studies has shown that signal correlation can degrade the system performance significantly in [4] and [5].

The adaptive transmit eigenbeamforming combined with orthogonal space-time block coding (OSTBC) for OFDM systems has been studied in [6] over macrocell environment where ULA was deployed at the base station (BS). The performance of this scheme is based on uplink angle-of-arrival (AoA) information. In this paper we further investigate the behavior of this adaptive transmission scheme over practical measurement data for macrocell and microcell environments. Moreover, the impact of different array configurations is also considered.

Notation used: $(\cdot)^*$, $(\cdot)^T$, and $(\cdot)^H$ are complex conjugate, vector transposition, and Hermitian transposition, respectively. $\|\cdot\|_F$ is the Frobenius norm; $\sqrt{\mathcal{A}}$ stands for Hermitian square root of matrix $\mathcal{A}$; Finally, capital (small) bold letters represent matrices (vectors).

II. SYSTEM MODEL

A general structure of the transmit scheme is shown in Fig. 1. It combines adaptive eigenbeamforming with orthogonal space-time block coding (Eigen-OSTBC) for broadband orthogonal frequency division multiplexing (OFDM). This system deploying N_t and N_r antennas at the transmitter and receiver, respectively. The OFDM system utilizes N_c frequency tones and the simulated channels are frequency-selective [7].
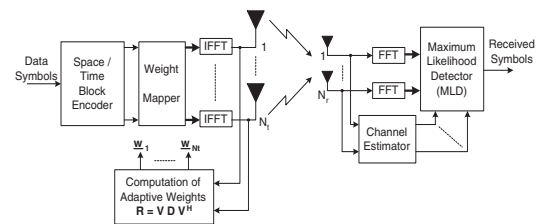

Fig. 1. General structure of the adaptive transmission scheme with OSTBC and eigenbeamforming.

At the BS, OSTBC is performed by formatting a sequence of baseband modulated data symbols into N_c codeword matrices before the linear transformation process of eigen weight mapping. Let us denote OSTBC output codeword for the kth subcarrier as $\mathbf{C}_k \in \mathbb{C}^{N_t \times N}$, which spans across N OFDM-symbol intervals and N_t transmit antennas. Since the number of baseband constellation points is finite, there is a limited number of possible OSTBC codeword matrices that can be generated per subcarrier and we denote this finite set as $\Upsilon_k \ni \mathbf{C}_k$. In this paper, the specific details of OSTBC construction are not described as we consider only the performance of the proposed transmission structure in different channel environ-

ment. We refer readers to [14], [15] for detailed description of formatting and decoding procedures of OSTBC.

A. Propagation Channel Models

In this Section, we provide general descriptions for the geometrical-based hyperbolically distributed scatterers (GB-HDS) channel models for macrocell and microcell environments [7], [8], [9]. A comprehensive study of these models (at theoretical and simulation levels) as well as their validation with practical data reported in [10], [11] and [12] have been considered. They proved to be more realistic than other models in the literature when tested against practical data [7], [8].

1) The GBHDS for Macrocell Environment: The GBHDS for macrocell environment channel model assumes that the scatterers are arranged within a circle of radius R around the mobile. The distances r between the mobile station (MS) and the scatterers are distributed according to the hyperbolic probability density function (pdf) [7]. The geometrical scatterer density function (GSDF) for this model, $f_r(r)$, is given by

$$f_r(r) = \begin{cases} \frac{a}{\tanh(aR)\cosh^2(ar)} & \text{for } 0 \leq r \leq R \\ 0 & \text{elsewhere} \end{cases} \quad (1)$$

where R is the radius of the circle enclosing the scatterers, and the applicable values of a lie in the interval (0,1) [7], [8]. The value of the parameter a controls the spread of the scatterers around the MS.

This model has been validated against measurement data reported in [10], [11]. In [10], Pedersen et al. conducted a number of outdoor measurement results, collected in a macrocell typical urban environment. These measurements were performed in Aarhus, Denmark and Stockholm, Sweden. From these results the statistics for the direction of arrival (DOA) and time of arrival (TOA) are measured. These measurements were conducted at 1.8 GHz carrier frequency, 4.096 Mcps chip rate (wideband CDMA), and at 122 ns sampling time. The angular histogram data of DOA had standard deviation of 7° while the delay histogram data for TOA had root mean squared delays of 0.682 μs. The results of the GBHDS channel model has shown that there was a good match between the model result and the measurement data reported in [10] for outdoor environment. In this paper the GBHDS model will be simulated with the same measurement angular spread (angluar spread of of 7°).

2) The GBHDS for Microcell Environment: The GBHDS for microcell environment is an extension of the macrocell model proposed in [7], however in this model the base station (BS) antenna is relatively low and multipath scattering near the BS is just as likely as multipath scattering near the mobile station (MS). Although in microcell environment there are two types of propagation: LOS and non-LOS propagation, this model assumes that there is a LOS path between the transmitter and the receiver and that the scatterers are arranged in a circle centered on the MS, with the circle radius being R. It is further assumed that the BS lies within this circle [9]. The distances, r, between the scatterers and the MS conform

to a hyperbolic distribution as in the macrocell scenario. The GSDF for this model is given by the same equation as in (1).

Validation of this model using practical data reported in [12] has been presented in [9]. In [12], Spencer *et al.* conducted a number of indoor measurement results, collected at 7 GHz within office buildings on the BYU campus. The scanning was done mechanically with a 6° horn over a 360° range. At the Clyde building, the angular data measured is for data within one cluster about its mean angle. The angular spread (standard deviations) is 24.5°. As this model shows a good match with measurement data, therefore in this paper we simulate this model with the same measurement angular spread (angular spread of of 24.5°).

B. Antenna Array Configurations

In this paper we study the performance of adaptive transmit eigenbeamforming with orthogonal space-time block coding over macrocell and microcell environments for different antenna array configurations. These array configurations are ULA and UCA (See figure 2).
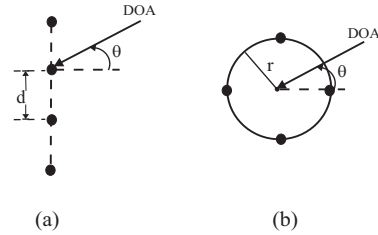

Fig. 2. Antenna array configurations: (a) uniform linear array (ULA) (b) uniform circular array (UCA).

We consider a base station (transmit antennas) equipped with an N_t identical and omnidirectional elements. In the following we will discuss the array response vectors at the DOA θ for different array geometries.

- Uniform Linear Array: The steering vector for ULA to an incoming signal from a DOA θ has the form:

$$\mathbf{a}(\theta) = [1, \, a_2(\theta), \, ..., \, a_{N_t}(\theta)]^T \quad (2)$$

where $a_{n_t}(\theta)$ is a complex number denoting the amplitude and the phase shift of the signal at the nth antenna relative to that at the first antenna. For a ULA, $a_{n_t}(\theta) = e^{[j2\pi(n_t-1)\,d\,\sin(\theta)/\lambda]}$, where d is the space between adjacent antennas, $n_t = 1, 2, \cdots, N_t$, and λ is the wavelength of the carrier.

- Uniform Circular Array: The steering vector for UCA to an incoming signal from a DOA θ has the form:

$$\mathbf{a}(\theta) = [a_1(\theta), \, a_2(\theta), \, ..., \, a_{N_t}(\theta)]^T \quad (3)$$

where $a_{n_t}(\theta)$ is given by, $a_{n_t}(\theta) = e^{[j2\pi\,r/\lambda\,\cos(\theta-2\pi(n_t-1)/N_t)]}$, where r is the radius of the array.

The normalized transmit spatial covariance matrix that specifies the spatial correlation between antenna elements is

defined as [13]

$$\mathbf{R}_t = \frac{1}{L} \sum_{\ell=1}^{L} \mathbf{a}(\theta_\ell) \mathbf{a}^H(\theta_\ell) , \qquad (4)$$

where L denotes the number of dominant resolvable paths (i.e., arriving signal paths that are more than one symbol length apart with significant received power). The spatial correlation at the receiver side is assumed to be zero (single antenna), hence, only the transmitter side will be considered. This means that $\mathbf{R}_r = \mathbf{I}_{N_r}$, where $\mathbf{I}_b$ is an identity matrix of size $b \times b$.

In general, $\mathbf{R}_t$ is a nonnegative-definite Hermitian matrix and its eigenvalue-decomposition (EVD) can be expressed as $\mathbf{R}_t = \mathbf{V}\mathbf{D}\mathbf{V}^H$, where $\mathbf{V} = [\boldsymbol{v}_1, \cdots, \boldsymbol{v}_{N_t}]$ is a unitary matrix with columns that are the eigenvectors of $\mathbf{R}_t$ and $\mathbf{D} = \text{diag}\{\mu_1, \mu_2, \cdots, \mu_{N_t}\}$ contains the corresponding eigenvalues. Define $\mathbf{g}_{i,j} = [g_{i,j}(0), \cdots, g_{i,j}(L-1)]$ as the L-tap channel impulse response vector for the $(i,j)^{\text{th}}$ receive-transmit antenna pair. The channel frequency response matrix can be expressed as $\mathbf{H}_k \in \mathbb{C}^{N_r \times N_t}$ with its $(i,j)^{\text{th}}$ entry $h_{i,j,k} = \mathbf{g}_{i,j}\mathbf{f}_k$ where $\mathbf{f}_k = [1, e^{-j2\pi(k-1)/N_c}, \cdots, e^{-j2\pi(k-1)\tau_{L-1}/N_c}]^T$ is the corresponding discrete Fourier transform coefficients and τ_ℓ is the integer delay of the ℓth tap. The correlated channel frequency response can then be given as $\mathbf{H}_k\sqrt{\mathbf{R}_t}$. We assume that the spatial correlation is the same for all subcarriers.

To facilitate OSTBC codeword transmission in the eigen-modes of the correlation matrix, eigen weight mapping is performed across the space dimension of the OSTBC codeword $\{\mathbf{C}_k\}_{k=1}^{N_c}$ prior to transmission. Mathematically, it can be expressed as $\mathbf{W}^H\mathbf{C}_k$, where $\mathbf{W} = [\mathbf{w}_1, \cdots, \mathbf{w}_{N_t}]$ is the eigen weight mapping matrix and $\mathbf{w}_j = \boldsymbol{v}_j$. Then signal transmission on different eigenvectors of $\mathbf{R}_t$ amounts for transmitting N_t orthonormal beams in the direction of the dominant multipaths seen by the BS. In the case when $\mathbf{R}_t$ is not the same for all subcarriers, beamforming should be performed individually for groups of subcarriers with one coherent bandwidth apart.

At the receiver, discrete Fourier transformation (DFT) is applied to the received signals from N_r antennas. The discrete time baseband equivalent expression of the received signal has the form

$$\mathbf{Y}_k = \mathbf{H}_k\sqrt{\mathbf{R}_t}\mathbf{W}^H\mathbf{C}_k + \mathbf{E}_k , \qquad (5)$$

where $\mathbf{E}_k$ is the receiver noise matrix and its elements are modelled as uncorrelated white Gaussian random variables having $\mathcal{N}(0, \sigma_n^2)$. At the receiver, channel estimation is performed by correlating pilot tones embedded in the transmitted signal. The result is then fed into the MLD for OSTBC codeword decoding of data symbols by evaluating the decision matrix as follows

$$\widehat{\mathbf{C}}_k = \arg \min_{\mathbf{C}_k \in \boldsymbol{\Upsilon}_k} \|\mathbf{Y}_k - \mathbf{H}_k\sqrt{\mathbf{R}_t}\mathbf{W}^H\mathbf{C}_k\|_F^2 . \qquad (6)$$

III. PERFORMANCE ANALYSIS: PAIRWISE ERROR PROBABILITY

Assuming that the receiver has perfect knowledge of the channel and that the decision matrix in (7) is evaluated at the MLD for symbol detection, the pairwise error probability (PEP) for an erroneous detection of the codeword $\widetilde{\mathbf{C}}_k$ in favor of $\mathbf{C}_k$ conditioned on the fading channel $\mathbf{H}_k = \{h_{i,j,k}\}_{i=1, \ j=1}^{N_r, \ N_t}$ can be expressed as

$$P_r(\mathbf{C}_k \to \widetilde{\mathbf{C}}_k \mid \mathbf{H}_k) = Q\left(\sqrt{\frac{d^2(\mathbf{C}_k, \widetilde{\mathbf{C}}_k)\,\rho}{2}}\right), \qquad (7)$$

where $\rho = \varepsilon_s/\sigma_n^2$, ε_s is the average symbol energy, $Q(\cdot)$ is the classical Gaussian Q-function, and $d^2(\mathbf{C}_k, \widetilde{\mathbf{C}}_k) := \|\mathbf{H}_k\sqrt{\mathbf{R}_t}\mathbf{W}^H(\mathbf{C}_k - \widetilde{\mathbf{C}}_k)\|_F^2$ is commonly known as the squared Euclidean distance between the two codeword matrices. Using the Chernoff bound in [16], (8) can be upper-bounded as

$$P_r(\mathbf{C}_k \to \widetilde{\mathbf{C}}_k \mid \mathbf{H}_k) \leq \exp\left(\frac{-d^2(\mathbf{C}_k, \widetilde{\mathbf{C}}_k)\,\rho}{4}\right). \qquad (8)$$

Defining $\mathbf{h}_{i,k} = [\mathbf{H}_k(i,1), \cdots, \mathbf{H}_k(i,N_t)] \in \mathbb{C}^{1 \times N_t}$ to be the ith row of $\mathbf{H}_k$. The squared Euclidean distance can then be rewritten as

$$d^2(\mathbf{C}_k, \widetilde{\mathbf{C}}_k) = \sum_{i=1}^{N_r} \mathbf{h}_{i,k}\boldsymbol{\Psi}\mathbf{h}_{i,k}^H, \qquad (9)$$

where

$$\boldsymbol{\Psi} = \sqrt{\mathbf{R}_t}\mathbf{W}^H\mathbf{B}_k\mathbf{B}_k^H\mathbf{W}\sqrt{\mathbf{R}_t}^H \in \mathbb{C}^{N_t \times N_t} \qquad (10)$$

is the *effective error distance* between two distinct codeword matrices and $\mathbf{B}_k = \mathbf{C}_k - \widetilde{\mathbf{C}}_k$. It is observed that $\boldsymbol{\Psi}$ is a non-negative definite Hermitian matrix, and thus, EVD of $\boldsymbol{\Psi}$ has a form of $\boldsymbol{\Lambda}\boldsymbol{\Psi}\boldsymbol{\Lambda}^H = \boldsymbol{\Omega}$, where $\boldsymbol{\Lambda}$ is a unitary matrix, $\boldsymbol{\Omega} = \text{diag}\{\omega_1, \cdots, \omega_r\}$ contains nonzero eigenvalues, and r is the rank of $\boldsymbol{\Psi}$. We assume that the elements of $\{\mathbf{h}_{i,k}\}_{i=1}^{N_r}$ are independent and identically distributed (i.i.d.) complex Gaussian random variables. By averaging the conditional PEP in (9) over all channel realizations, the PEP of an Eigen-OSTBC OFDM system can be finally written as

$$P_r(\mathbf{C}_k \to \widetilde{\mathbf{C}}_k) \leq \left(\prod_{m=1}^{r} \omega_m\right)^{-N_r}\left(\frac{\gamma}{4}\right)^{-rN_r}, \qquad (11)$$

where $\gamma = \rho\|\sqrt{\mathbf{R}_t}\mathbf{W}^H\|_F^2$ denotes the effective receiver SNR. Then the array weighting gain (AWG) of this system over systems without beamforming can be found as $\sum_{j=1}^{N_t} \mathbf{w}_j\mathbf{R}_t\mathbf{w}_j^H$.

Equivalently, the AWG can also be expressed as $\sum_{\ell=1}^{L} \mu_\ell$, sum of eigenvalues of the spatial correlation matrix. In [5], it is shown that the AS of arriving multipaths can strongly affect the distribution of this eigenvalues and hence the AWG of our transmission structure. In the next Section, we will use computer simulation to demonstrate the effect of different multipath AS and antenna array configuration have on the error performance of the transmission structure by using actual experiential measurement data from various propagation environment.

IV. NUMERICAL RESULTS AND DISCUSSION

In this Section, we provide bit-error-rate (BER) and symbol-error-rate (SER) performance curves of adaptive broadband OFDM systems frequency-selective channels with different propagating environments. In the simulation conducted, the following system parameters and assumption were adopted: QPSK is used for baseband modulation of information data, the spatial channel correlation is modelled using GBHDS channel model in [7], [8], [9], $\mathcal{G}_4$ encoding matrix in [14] is utilized for OSTBC codeword construction, and hence $N_t = 4$, $N_r = 1$, and $N_c = 512$ were employed for the OFDM system.

In Figs. 3 and 4, we first demonstrated the performance improvement of using the Eigen-OSTBC systems over systems using only OSTBC in a correlated channel environment. The ULA and UCA antenna configurations were used at the BS to simulate the results in Fig. 3 and 4, respectively. It is clearly shown that there is a significant performance difference between this two transmission schemes in the same channel condition (macrocell environment with AS = $7°$), where the difference gets larger as the SNR increases. It is also evident that the transmit antenna configuration has influenced the performance of the system. From these figures, the UCA configuration has a better performance than the ULA config-uration.
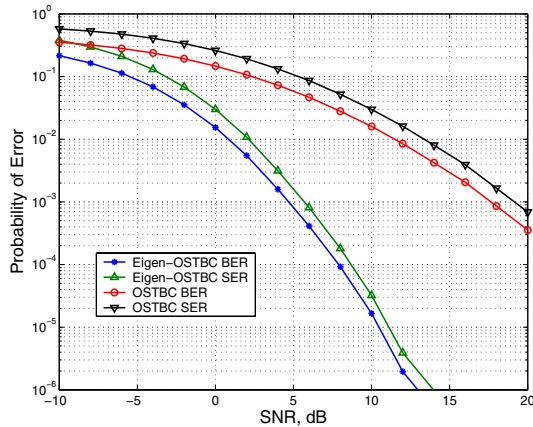

Fig. 3. Simulated error rate performance of the OSTBC and OSTBC-Eigen OFDM systems over GBHDS macrocell channel model deploying ULA antenna at the transmitter with $d = 0.5\lambda$.

Figs. 5 and 6 shows the performance of the Eigen-OSTBC systems over the GBHDS macrocell and microcell channel models (macrocell environment with AS = $7°$ and microcell environment with AS = $24.5°$) deploying ULA and UCA antenna configurations at the transmitter, respectively. It is clearly shown that the Eigen-OSTBC system has better performance in macrocell channel environment since the AS is smaller, and thus, these results collaborated with the AWG shown in the previous Section. In these figures the ULA has a slightly better performance than the UCA configuration.

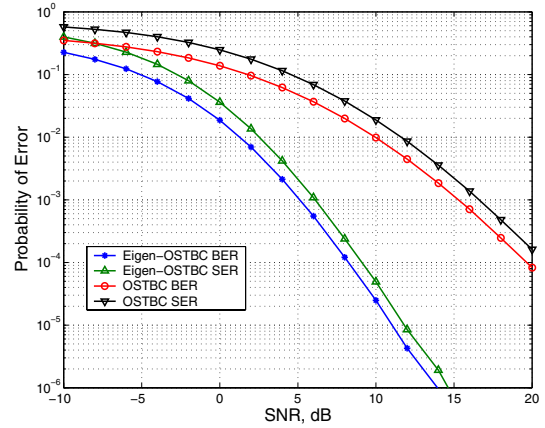Figs. 7 and 8 show the performance of the OSTBC systems over the GBHDS macrocell and microcell channel models

Fig. 4. Simulated error rate performance of the OSTBC and OSTBC-Eigen OFDM systems over GBHDS macrocell channel model deploying UCA antenna at the transmitter with $r = 1.4\lambda$.
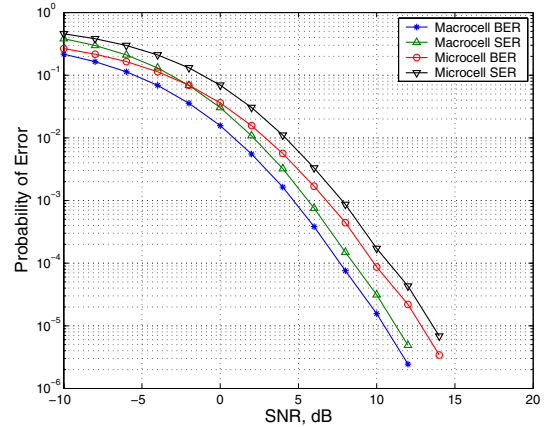

Fig. 5. Simulated error rate performance of the OSTBC-Eigen OFDM system over GBHDS macrocell and microcell channel models deploying ULA antenna at the transmitter with $d = 0.5\lambda$, AS for microcell channel = $24.5°$ and AS for macrocell channel = $7°$.
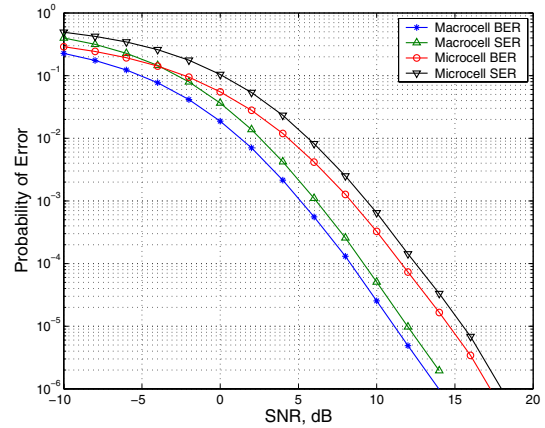

Fig. 6. Simulated error rate performance of the OSTBC-Eigen OFDM system over GBHDS macrocell and microcell channel models deploying UCA antenna at the transmitter with $r = 1.4\lambda$, AS for microcell channel = $24.5°$ and AS for macrocell channel = $7°$.

(macrocell environment with AS = $7°$ and microcell environment with AS = $24.5°$) deploying ULA and UCA antenna configurations at the transmitter, respectively. It is clearly shown that the OSTBC systems without eigenbeamforming has better performance in microcell channel environment than in macrocell channel environment. This improvement is obviously observed when SNR increases. This is due to the wider AS in microcell environment relative to that in macrocell, and hence less spatial correlation in the transmitted signal.
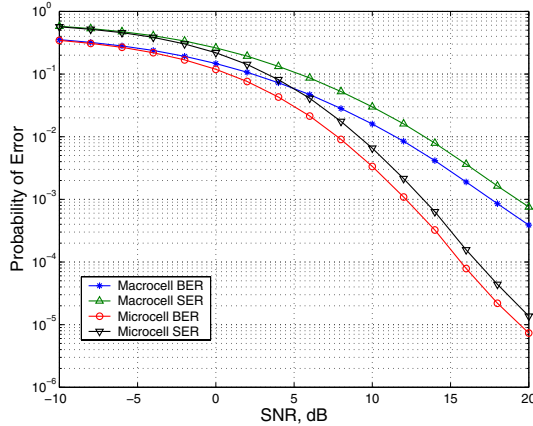
Fig. 7. Simulated error rate performance of the OSTBC OFDM system over GBHDS macrocell and microcell channel models deploying ULA antenna at the transmitter with $d = 0.5\lambda$, AS for microcell channel = $24.5°$ and AS for macrocell channel = $7°$.
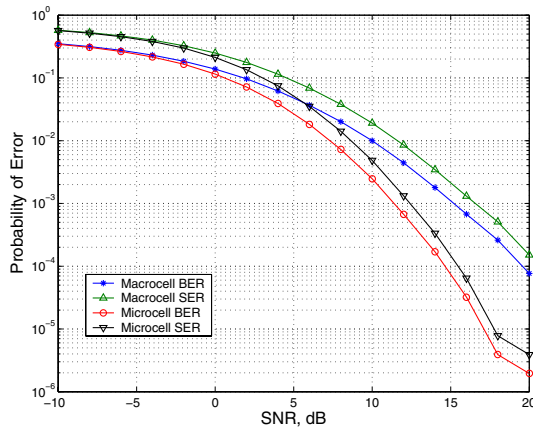
Fig. 8. Simulated error rate performance of the OSTBC OFDM system over GBHDS macrocell and microcell channel models deploying UCA antenna at the transmitter with $r = 1.4\lambda$, AS for microcell channel = $24.5°$ and AS for macrocell channel = $7°$.

V. CONCLUSION

In this work, we investigated the error-rate performance of an adaptive OFDM system employing transmit eigenbeam-forming and orthogonal space-time block coding schemes for multi-antenna system in various channel environment. It is shown that an array weighting gain (AWG) is strongly related to the angle spread (AS) of the channel, and our simulation results demonstrated a higher performance improvement when the system is operating in macrocell environment as compared to microcell where multipaths AS is much larger.

REFERENCES

[1] G. J. Foschini and M. J. Gans, "On limits of wireless communications in a fading environment when using multiple antennas," *Wireless Pers. Commun.*, vol. 6, no. 3, pp. 311-335, Mar. 1998.

[2] V. Tarokh, N. Seshadri, and A. R. Calderbank, "Space-time codes for high data rate wireless communication: Performance criterion and code construction," *IEEE Trans. Inform. Theory*, vol. 44, pp. 744-764, Mar. 1998.

[3] V. Tarokh, H. Jafarkhani, and A. R. Calderbank, "Space-time block coding for wireless communications: Performance results," *IEEE J. Select. Areas in Commun.*, vol. 17, pp. 451-460, Mar. 1999.

[4] D-S. Shiu, G. J. Foschini, M. J. Gans, and J. M. Khan, "Fading correlation and its effect on the capacity of multielement antenna systems," *IEEE Trans. Commun.*, vol. 48, pp. 502-513, Mar. 2000.

[5] H. Bolcskei and A. J. Paulraj, "Performance of space-time codes in the presence of spatial fading correlation," in *Proc. 34th Asilomar Conf. on Signals, Systems and Computers*, vol. 1, 2000, pp. 687-693.

[6] K. H. Lin, Z. M. Hussain, and Richard J. Harris, "Space-Time OFDM with Adaptive Beamforming: Performance in Spatially Correlated Channels," *IEEE TENCON'04*, Chiang-Mai, Nov. 2004, pp. 617-620.

[7] S. S. Mahmoud, Z. M. Hussain, and P. O'Shea, "A Geometrical-Based Channel Model with Hyperbolically Distributed Scatterers for a Macrocell Mobile Environment with Antenna Array," *Multimedia Cyberscape Journal*, vol. 2, pp.1-10, 2004.

[8] S. S. Mahmoud, Z. M. Hussain, and Ajit Gopalakrishnan, "Spatial and Temporal Statistics for the Geometrical-Based Hyperbolic Macrocell Channel Model," *Submitted to IEEE Transactions on Vehicular Technology*.

[9] S. S. Mahmoud, Z. M. Hussain, and Peter O'Shea, "A Multipath Mobile Channel Model for Microcell Environment," *IEEE International Symposium on Spread Spectrum Techniques and Applications,* Australia, Sept. 2004.

[10] K. I. Pedersen, P. E. Mogensen, and B. Fleury, "A stochastic model of the temporal and azimuthal dispersion seen at the base station in outdoor propagation environments," *IEEE Trans. Veh. Technol.*, vol. 49, pp. 437447, March 2000.

[11] R. Janaswamy, "Angle and Time of Arrival Statistics for the Gaussian Scatter Density Model," *IEEE Transactions on Wireless Communications*, vol. 1, No. 3, pp. 488-497, July 2002.

[12] Q. H. Spencer, B. D. Jeffs, M. A. Jensen, and A. L. Swindlehurst, "Modeling the Statistical Time and Angle of Arrival Characteristics of an Indoor Multipath Channel," *IEEE Journal on Selected Areas in Communications*, vol. 18, NO. 3, pp. 347-360, Mar. 2000.

[13] Siemens, *Channel Model for Tx Diversity Simulations using Correlated Antennas*, 3GPP Document TSG-RAN WG1 #15, R1-00-1067, Berlin, Germany, Aug. 2000.

[14] V. Tarokh, H. Jafarkhani, and A. R. Calderbank, "Space-time block codes from orthogonal designs," *IEEE Trans. Inform. Theory*, vol. 45, pp. 1456-1467, July 1998.

[15] V. Tarokh, H. Jafarkhani, and A. R. Calderbank, "Space-time block coding for wireless communications: Performance results," *IEEE J. Select. Areas in Commun.*, vol. 17, pp. 451-460, Mar. 1999.

[16] J. G. Proakis, *Digital Communications*, New York, N.Y.: McGraw-Hill Inc., Fourth Edition, 2001.